Infrared Action Spectroscopy of the OD Stretch Fundamental and Overtone Transitions of the DOOO Radical†

Erika L. Derro, Timothy D. Sechler, Craig Murray, and Marsha I. Lester*

Department of Chemistry, University of Pennsylvania, Philadelphia, Pennsylvania 19104-6323

Received: February 11, 2008; Revised Manuscript Received: March 24, 2008

The DOOO radical has been produced by three-body association between OD and O_2 in a supersonic free-jet expansion and investigated using action spectroscopy, an IR−UV double-resonance technique. Partially rotationally structured bands observed at 2635.06 and 5182.42 cm^{-1} are assigned to the OD stretch fundamental (ν_{OD}) and overtone ($2\nu_{OD}$), respectively, of the *trans*-DOOO radical. Unstructured bands observed in both spectral regions are assigned to *cis*-DOOO. Nascent OD $X^2\Pi$ product state distributions following vibrational predissociation appear to be nearly statistical with respect to the degree of rotational excitation, but display a marked propensity for $\Pi(A')$ Λ-doublets, which is interpreted as a signature of a planar dissociation. The energetically highest open OD $X^2\Pi$ product channel implies an upper limit dissociation energy $D_0 \leq 1856$ cm^{-1} or 5.31 kcal mol^{-1}. This value allows refinement of the upper limit D_0 of the atmospherically important HOOO isotopomer, suggesting that it is marginally less stable than previously thought.

1. Introduction

The HOOO radical is an important reactive intermediate in both gas- and solution-phase chemical and biological processes. There is evidence that it plays a role in the antibody-catalyzed oxidation of water in bactericidal pathways,[1,2] is involved in the ozonation of organic species,[3–5] in the peroxone reaction used in water treatment,[6] and in several important atmospheric processes. In the atmosphere, two examples in which an HOOO intermediate has been invoked are the reaction between hydrogen atoms and ozone,[7,8] which generates vibrationally excited hydroxyl radicals responsible for airglow in the mesosphere,[9] and the reaction between oxygen atoms and hydrogen peroxy radicals. The kinetics of vibrational relaxation of OH by O_2 is also predicted to be controlled by intramolecular vibrational energy redistribution (IVR) in the HOOO intermediate.[10–13] Interest in the role of HOOO in the atmosphere has also led to consideration of the equilibrium:[14–16]

$$OH + O_2 \rightleftharpoons HOOO \qquad (1)$$

If HOOO is sufficiently stable relative to the OH + O_2 asymptote, significant amounts of HOOO could exist in the atmosphere and thus provide a temporary sink for hydroxyl. In light of this importance, there have been many theoretical studies and a few experimental investigations of HOOO, but there remain significant discrepancies between experiment and theory with respect to its structural properties and stability.

Early theoretical investigations of HOOO predicted three minimum energy structures, *cis*-, *trans*-, and *perp*-HOOO.[15,17–19] Contemporary calculations have brought about the consensus that only cis and trans, both of which are planar, are true minima.[20–26] However, a large disparity remains in the theoretical literature as to which conformer represents the global minimum and, more importantly, their stability relative to OH + O_2. One of the major difficulties in theoretical treatments of HOOO is the multiconfigurational nature of the ground state which results in the failure of most commonly used single-reference ab initio methods to predict geometries reliably with obvious consequences for thermochemical calculations using established model chemistries. The geometrical disparities are most dramatically evidenced in the length of the central OO bond, with reported bond lengths ranging from ∼1.4 to ∼1.7 Å.[21] The nature of the bonding in HOOO has recently been investigated theoretically using the atoms-in-molecules (AIM) formalism by Mansergas et al. and led to the suggestion that the central OO bond is not a true covalent interaction.[27]

Experimental data on HOOO have been relatively sparse since its first detection by Cacace et al. using neutralization−reionization mass spectrometry.[14] HOOO has since been detected in H_2O/O_2 ice mixtures[28,29] as well as in an Ar matrix by Nelander et al. who assigned some vibrational frequencies for HOOO via comparison to its isotopically substituted analogues.[30] Work by Suma et al. using Fourier transform microwave (FTMW) spectroscopy yielded observations of rotational transitions for both HOOO and DOOO in the gas phase, from which structures and rotational constants of *trans*-HOOO and DOOO were derived.[16] Until recently, the only experimental measurement of the stability came from work by Speranza, who inferred a standard heat of formation for HOOO of -1 ± 5 kcal mol^{-1} from the electron transfer efficiency of its cation.[31,32] This value has since been refined by experiments in our laboratory using IR action spectroscopy which set an upper limit on the dissociation energy, $D_0 \leq 2140$ cm^{-1} or 6.12 kcal mol^{-1}. A statistical mechanical analysis using this upper limit D_0 indicated HOOO may be a significant sink for OH in the vicinity of the tropopause.[33] In addition, our work has shown that, in both the fundamental and overtone of the OH stretch, there are two features in the IR spectrum: a rotationally structured band which was assigned to *trans*-HOOO and an unstructured feature which was assigned to *cis*-HOOO.[34]

The limit on the dissociation energy set by the aforementioned experiments was determined by probing the nascent OH $X^2\Pi$ products of vibrational predissociation using laser-induced fluorescence−excitation spectroscopy following excitation of the OH stretch of HOOO.[33,34] This state-selective approach

† Part of the "Stephen R. Leone Festschrift".

* To whom correspondence should be addressed. Phone: (215) 898-4640. Fax: (215) 573-2112. E-mail: milester@sas.upenn.edu.

10.1021/jp801232a CCC: $40.75
Published on Web 05/29/2008

allowed determination of the energetically highest open OH product channel, and then a straightforward conservation of energy approach was applied to calculate D_0. It should be noted that, in the more populated F_1 spin−orbit manifold, the next highest OH rotational level lies ~300 cm^{-1} higher in energy;[35] therefore, the precision of the measurement was inherently limited by the spacing between adjacent energetic levels in addition to the detection sensitivity.

The deuterated isotopomer, DOOO, may provide a means to refine the upper limit on the dissociation energy, as the energetic spacing between the rotational levels of OD is smaller than for OH.[36] An accurate measurement of this value is essential because estimations of atmospheric abundance of HOOO from statistical mechanical calculations are extremely sensitive to the value of D_0. Examination of DOOO could also provide further insight to the origin of the unstructured features observed in the OH stretch fundamental and overtone spectra of HOOO, which have been assigned to the cis conformer, as they would be expected to display appropriate isotopic shifts upon deuteration. Here, we report infrared action spectra of the fundamental and overtone OD stretch transitions for both *cis*- and *trans*-DOOO and discuss the dynamics of the subsequent vibrational predissociation. In addition we determine the upper limit of the dissociation energy of DOOO and evaluate the implications this has on the D_0 of HOOO.

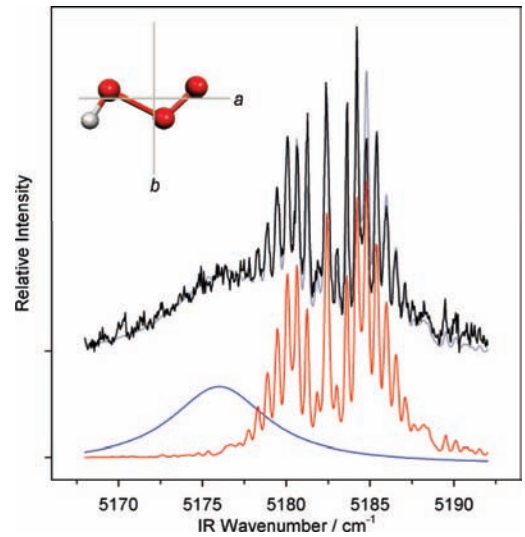

Figure 1. Experimental IR action spectra (black) of the DOOO radical in the OD stretch overtone region recorded with the UV probe laser fixed on the $P_1(5)$ transition of the OD $A^2\Sigma^+-X^2\Pi$ (1,1) band. The total simulation (gray) is the sum of the rotationally structured band (red) assigned to *trans*-DOOO and unstructured band (blue) assigned to *cis*-DOOO as discussed in the text. The structure of *trans*-DOOO in the principal axis system is also shown.

2. Experimental Section

The experimental setup is comparable to the method previously used for production of HOOO radicals in this laboratory and has been described in detail elsewhere.[33,34] Briefly, DOOO radicals are generated following the three-body association of OD radicals and O_2 in the collisional region of a pulsed free-jet expansion. The OD radicals are produced directly beyond the aperture of the pulsed valve by photolysis of $DONO_2$ (98% D, 90% in D_2O, Isotec, Inc.) seeded in a mixture of O_2 (20% by volume) and Ar (balance) at a backing pressure of 35 psi, using the 193 nm output of an ArF excimer laser (Lambda Physik Compex 102). DOOO radicals are subsequently formed and stabilized by collisions with the carrier gas.

IR action spectra of DOOO and the nascent OD $X^2\Pi$ product state distributions following vibrational predissociation were recorded using an IR pump−UV probe technique. Tunable IR radiation of 0.15 cm^{-1} bandwidth, generated in an optical parametric oscillator (OPO, LaserVision), pumped by an injection-seeded Nd:YAG laser (Continuum Precision II 8000, 10 Hz), was used to excite either the OD stretch fundamental (ν_{OD}) or overtone ($2\nu_{OD}$) transition in DOOO at either ~3.80 or ~1.93 μm, respectively, causing dissociation to OD and O_2. After a delay of 50 ns, the nascent OD $X^2\Pi$ products of vibrational predissociation were probed by saturated laser-induced fluorescence (LIF) using the frequency-doubled output of a Nd:YAG pumped dye laser (Continuum Surelite II and ND6000, 20 Hz). The IR and UV laser beams are counterpropagating and spatially overlapped intersecting the expansion approximately $x/D = 15$ nozzle diameters downstream ~20 μs after photolysis and, thus, probe rotationally cold DOOO radicals.

The probe laser state-selectively excites OD on specific $A^2\Sigma^+-X^2\Pi$ transitions: (1,0) at ~288 nm following ν_{OD} excitation or (1,1) at ~312 nm following $2\nu_{OD}$ excitation. The resulting fluorescence was then collimated and refocused through a 1 mm wide slit before impinging upon a photomultiplier tube (Electron Tubes 9813QB) to ensure that the colder central region of the free-jet was imaged. Narrowband interference filters prior to the photomultiplier were also used to achieve wavelength discrimination and suppress scattered light from the probe laser. The signal from the photomultiplier was preamplified and displayed on a digital storage oscilloscope (LeCroy WaveRunner 6050A) interfaced with a PC for further processing.

The frequency of the unused signal wave from the oscillator stage of the OPO was continuously monitored using a wavemeter (Coherent Wavemaster) which, in combination with knowledge of the absolute frequency of the pump beam, allowed for calibration of the infrared laser frequency while recording spectra. It was necessary to purge the IR beam path with N_2 while recording the $2\nu_{OD}$ IR spectrum of DOOO to avoid water absorption in the 1.9 μm region.

3. Results

IR action spectra were recorded by scanning the frequency of the IR pump laser in the vicinity of the free OD stretch overtone and fundamental, while measuring the UV probe laser-induced signal on a selected OD $A^2\Sigma^+-X^2\Pi$ transition. Fluorescence arising from residual OD $X^2\Pi$ present in the expansion was subtracted on a shot-to-shot basis. This background population is predominantly confined to the lowest rotational levels of both $v = 0$ and $v = 1$, although a small residual high-N tail persists. The IR-induced LIF signals giving rise to the spectra shown in Figures 1 and 2 required O_2 to be present in the free-jet expansion and depended on the presence of the photolysis laser and are thus assigned to the OD stretch overtone and fundamental of DOOO. No IR-induced signal was observed when the UV laser preceded the IR but increased rapidly to a maximum when temporally overlapped indicating that the IR absorbing species dissociates to produce OD $X^2\Pi$ on a shorter time scale than the laser pulse widths, viz. <8 ns. The nascent OD $X^2\Pi$ product state distributions following vibrational predissociation of the vibrationally excited DOOO were also measured and analyzed to provide information on the relative stability of the DOOO radical and the dissociation dynamics.

3.A. OD Stretch Overtone. The OD stretch overtone spectrum of DOOO, shown in Figure 1, was recorded with the UV

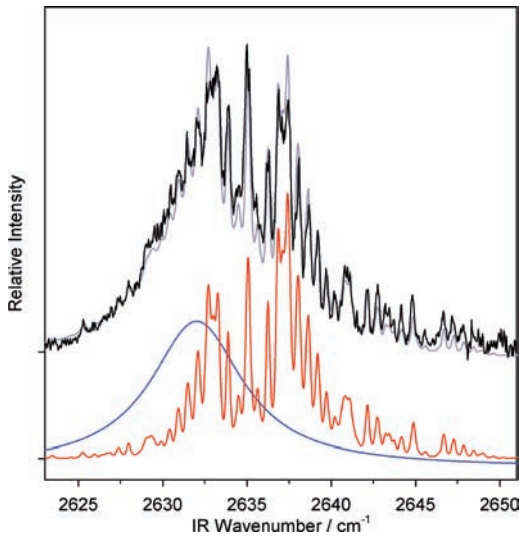

Figure 2. Experimental IR action spectra (black) of the DOOO radical in the OD stretch fundamental region recorded with the UV probe laser fixed on the $P_1(5)$ transition of the OD $A^2\Sigma^+ - X^2\Pi$ (1,0) band. The total simulation (gray) is the sum of the rotationally structured band (red) assigned to *trans*-DOOO and unstructured band (blue) assigned to *cis*-DOOO as discussed in the text.

probe laser fixed on the $P_1(5)$ transition of the A−X(1,1) band, which was found to result in the optimal signal-to-background ratio. The use of different OD A−X probe transitions leaves the IR spectra unchanged except for poorer signal-to-noise ratios. The overtone spectrum comprises a rotationally structured band at 5182.42 ± 0.05 cm^{-1} (origin, obtained from a fit described below) and an unstructured band centered at 5176.0 cm^{-1}. The structured band is blue-shifted by +6.90 cm^{-1} from the free OD overtone[36] at 5175.52 cm^{-1}, as summarized in Table 1 alongside the analogous values for HOOO. The overtone spectrum of DOOO was decomposed into two components iteratively, by simulating the rotationally structured band as described below and modeling the unstructured band using a Lorentzian function to obtain the best agreement with the experimental spectrum.

Previously, we observed a strikingly similar OH stretch overtone spectrum of HOOO[33,34] and assigned the rotationally structured band to the trans conformer and the unstructured band to the cis conformer. The rotationally structured band was assigned to *trans*-HOOO following the FTMW work of Suma et al.[16] who derived molecular constants for *trans*-HOOO and *trans*-DOOO from the pure rotational spectrum. The assignment of the observed microwave transitions to the trans conformers was made for two reasons. First, the magnitudes of the experimental rotational constants for both isotopomers were closer to those predicted for trans by high-level multireference ab initio calculations of the optimized geometries. Second, *a*-type and *b*-type transitions in the microwave spectrum were of similar intensity, consistent with the ab initio predicted projections of the permanent dipole moment of the trans conformer on the inertial axes. In contrast, the cis conformer would be expected to show principally *b*-type rotational transitions.

As found for HOOO,[34] simulation of the rotationally structured band of DOOO as an asymmetric top[37] using the FTMW rotational constants[16] for both the ground and vibrationally excited state reproduces the line positions and intensities exceptionally well. The agreement between the observed and calculated spectra deteriorates slightly using the ab initio rotational constants for *trans*-DOOO and significantly using those predicted for *cis*-DOOO.[16] Consequently, we assign the structured band to the OD stretch overtone of the *trans*-DOOO conformer. The simulated spectrum is also shown in Figure 1. Higher-order centrifugal distortion and fine-structure constants were also determined from the high-resolution FTMW work, but their inclusion produced no discernible difference to the simulations at the resolution of these experiments, which is limited by homogeneous (lifetime) broadening of the spectral lines.

The simulation of the $2\nu_{OD}$ band of *trans*-DOOO was optimized using a least-squares fitting procedure that treated the band origin, rotational temperature, Lorentzian component of the spectral line width, and the ratio of the *a* and *b* components of the transition dipole moment as variable parameters. A rotational temperature of ∼8 K was achieved in the region of the supersonic free-jet expansion intersected by the pump and probe laser beams. The spectral resolution is limited by homogeneous broadening beyond the resolution of the IR laser bandwidth (Gaussian with 0.15 cm^{-1} fwhm) that requires the inclusion of a Lorentzian component in the spectral lines in the simulation. The IR-enhanced fluorescence signal intensity was found to vary linearly with IR laser power, indicating that the broadening was not attributable to optical saturation of the vibrational transition. The fit to the overtone spectrum yielded a Lorentzian line width of 0.16 ± 0.01 cm^{-1} (2σ uncertainty), which corresponds to a lifetime of 33 ± 2 ps for the $2\nu_{OD}$ state of *trans*-DOOO. The lifetime broadening in the excited state of *trans*-DOOO is the result of either IVR and/or vibrational predissociation. Time domain measurements indicate that predissociation occurs on a shorter time scale than the laser pulse width which is consistent with the observation of broadened spectral lines.

The transition type of the *trans*-DOOO overtone spectrum is predominantly parallel, or *a*-type, which results in characteristic P-, Q-, and R-branch structure. A weaker contribution from *b*-type transitions produces distinct features further from the band origin. The integrated *a*/*b* intensity ratio $I_a/I_b = 4.6 \pm 0.5$, which is obtained from the fit to the experimental spectrum can be used to derive the ratio of the projections of the transition dipole moment on the *a* and *b* inertial axes, $\boldsymbol{\mu}_a/\boldsymbol{\mu}_b = 2.1 \pm 0.2$. Using the geometry for *trans*-DOOO obtained from the FTMW work of Suma et al.,[16] the transition dipole moment for the overtone transition lies 38° from the OD bond axis toward the *a*-axis. The structure of *trans*-DOOO in the principal axis system is shown as an inset in Figure 1.

The unstructured feature is assigned to excitation to $2\nu_{OD}$ of *cis*-DOOO in direct analogy to the similar feature observed in our previous work on HOOO. The band is well-represented by a Lorentzian with a full width at half-maximum (fwhm) of 7.0 cm^{-1}, which is similar to the breadth of the rotationally structured *trans*-DOOO band, and suggests the absorbing species has similar rotational constants. Alternatively, the unstructured band can be modeled by broadening a simulation using ab initio *cis*-DOOO rotational constants. A Lorentzian component of 4−5 cm^{-1} is sufficient to wash out the rotational structure, and would correspond to an excited-state lifetime on the order of ∼1 ps. The *cis*-DOOO band accounts for 33% of the total integrated intensity observed in the overtone region, when using the $P_1(5)$ probe transition.

3.B. OD Stretch Fundamental. The IR action spectrum shown in Figure 2 is assigned to the OD stretch fundamental of DOOO and was recorded with the UV probe fixed on the $P_1(5)$ transition of the OD A−X(1,0) band. Qualitatively, the spectrum is similar to the overtone, comprising two major

TABLE 1: Measured Band Origins and Shifts (in Parentheses) from Free OD and OH for the Cis and Trans Conformers of HOOO and DOOO in cm^{-1}

	DOOO		HOOO[a]	
	ν_{OD}	$2\nu_{OD}$	ν_{OH}	$2\nu_{OH}$
trans	2635.06 (+3.52)	5182.42 (+6.90)	3569.30 (+0.83)	6974.18 (+2.83)
cis	2632.0 (+0.5)	5176.0 (+0.5)	3565.4 (−3.1)	6968.3 (−3.1)
free OD/OH[b]	2631.54	5175.52	3568.47	6971.35

[a] Data from refs 33 and 34. [b] Data from refs 35 and 36.

features: a rotationally structured band at 2635.06 cm^{-1} (origin), which is assigned to the *trans*-DOOO conformer, and an unstructured band centered around 2632.0 cm^{-1}, which is assigned to *cis*-DOOO. The rotationally structured band was again assigned to *trans*-DOOO based upon the superior agreement with simulations using the FTMW rotational constants[16] and is blue-shifted by +3.52 cm^{-1} from the free OD fundamental[36] at 2631.54 cm^{-1} (see Table 1). The experimental fundamental spectrum was iteratively decomposed into its two contributing bands in the same manner as the overtone. The fit to the rotationally structured band also yielded a rotational temperature of ~8 K, and a Lorentzian line width of 0.16 ± 0.01 cm^{-1}, indicating no measurable difference in the rate of vibrational predissociation and/or IVR following excitation of ν_{OD} or $2\nu_{OD}$.

The OD stretch fundamental of *trans*-DOOO displays a rotational band contour which is distinctly different from the overtone. Hybrid band structure is apparent with approximately equal *a*-type and *b*-type contributions for the fundamental, whereas the overtone was predominantly *a*-type. The *a*/*b* integrated intensity ratio of the fundamental is quantified in the least-squares fitting procedure, yielding $I_a/I_b = 1.4 \pm 0.1$, and thus the ratio of the projections of the transition dipole moment is $\boldsymbol{\mu}_a/\boldsymbol{\mu}_b = 1.2 \pm 0.1$. The transition dipole moment is rotated 23° away from the OD bond toward the *a*-axis for the fundamental transition.

The unstructured *cis*-DOOO feature accounts for 47% of the integrated intensity in the fundamental region using the $P_1(5)$ probe transition and is thus relatively more intense than in the overtone region. The width of 6.7 cm^{-1} of the Lorentzian used to model the *cis*-DOOO fundamental is similar, however.

3.C. Product State Distributions. In addition to IR action spectra, the nascent OD $X^2\Pi$ product state distributions following vibrational predissociation of the ν_{OD} and $2\nu_{OD}$ excited *trans*-DOOO were recorded. The IR pump laser frequency was fixed on the R(3) features of the OD stretch fundamental and overtone spectra at 2637.4 and 5184.3 cm^{-1}, respectively, while the UV probe laser was scanned over individual OD A−X transitions, probing the nascent product population with rotational and fine-structure resolution. In addition to being among the most intense features in the spectra, IR excitation in the R-branches also provides good discrimination between the structured and unstructured components. The product state distribution was also measured with the IR pump laser frequency resonant with the unstructured *cis*-DOOO overtone feature at 5175.6 cm^{-1}; since the OH $X^2\Pi$, $v = 0$ and 1 product state distributions following ν_{OH} and $2\nu_{OH}$ excitation of *cis*-HOOO, respectively, were essentially identical, only the overtone was investigated.

Following fundamental excitation, product population was observed in OD $X^2\Pi$, $v = 0$ by exciting on specific transitions of the off-diagonal A−X(1,0) band and collecting the dominant diagonal (1,1) fluorescence. The fluorescence scheme was simply inverted when detecting OD $X^2\Pi$, $v = 1$ dissociation products arising from overtone excited DOOO. No product

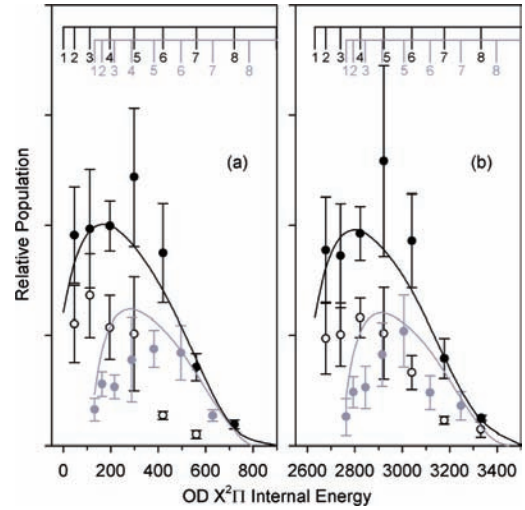

Figure 3. Nascent product state distributions displayed as a function of internal energy for (a) OD $X^2\Pi$ $v = 0$, arising from vibrational predissociation of *trans*-DOOO after excitation at 2637.44 cm^{-1} and (b) OD $X^2\Pi$ $v = 1$, arising from vibrational predissociation of *trans*-DOOO after excitation at 5184.25 cm^{-1}. The ticks identify OD rotational levels. Black and gray circles are used to represent population the F_1 and F_2 spin−orbit manifolds, respectively; filled circles are used for Π(A′), and open circles are used for Π(A″) Λ-doublet levels. The error bars represent 2σ uncertainties from repeated measurements. The solid lines represent prior distributions that provide the best fit to the data.

population was observed in OD $X^2\Pi$, $v = 0$ following excitation of the overtone. For a given rotational level, *N*, there are four fine-structure substates which, in the high-*J* limit, correspond to Π(A′) or Π(A″) Λ-doublet levels within both the F_1 and F_2 spin−orbit manifolds. For the most part, fine-structure-resolved detection is straightforward, as P- and R-type main branch transitions originate from Π(A′) levels, whereas Q-type main branch transitions originate from Π(A″) levels. The intensities were determined from the amplitudes of least-squares fits of the spectral lines, which were typically recorded in batches of four and scaled relative to a selected reference transition. Each batch was repeated multiple times to determine the statistical uncertainty in the signal intensities. Conversion to relative populations was performed using a saturated LIF analysis procedure, described in detail previously,[38] which incorporates the fluorescence wavelength-dependent detection sensitivity, the fluorescence quantum yields, and degeneracy correction factors.

Figure 3 shows the OD $X^2\Pi$ product state distributions as a function of internal energy observed following IR excitation of the *trans*-DOOO fundamental and overtone. The distributions observed in $v = 0$ and $v = 1$ are remarkably similar, despite arising from excitation of one and two quanta of OD stretch, respectively. In the ground F_1 spin−orbit manifold, the rotational distributions peak in $N = 5$ ($J = {}^{11}/_2$), showing a marked preference for production of Π(A′) Λ-doublets over Π(A″). This effect is manifest in the significantly greater intensity of P_1 over Q_1 transitions. The $N = 5$ ($J = {}^{9}/_2$) level is also the most

populated in the excited F_2 manifold. The population distribution in $\Pi(A'')$ Λ-doublets was not examined for rotational levels within F_2. However, by analogy with the vibrational predissociation of $2\nu_{OH}$ excited *trans*-HOOO, it is anticipated that the greater part of the population has been observed in the $\Pi(A')$ Λ-doublets. The relative populations in the F_1 and F_2 spin−orbit manifolds indicate no propensity, once corrected for the different degeneracies of levels with the same value of N.

Rotational distributions calculated using phase-space theory indicate an absence of angular momentum constraints in the unimolecular dissociation of DOOO but were otherwise in relatively poor agreement with those observed. The rotational population distributions observed for the $\Pi(A')$ levels in the F_1 and F_2 spin−orbit manifolds of $v = 0$ and $v = 1$ were modeled more simply by fitting to a prior distribution, for a fixed total energy. The excess energy, E_{exc}, available to the OH and O_2 products, i.e., the IR photon energy minus the dissociation energy, and an overall scaling factor were variable parameters. The prior distribution was constrained to populate only $v = 1$ when fitting the product state distribution measured following *trans*-DOOO overtone excitation. The best-fit distributions are presented as lines through the experimental data in Figure 3. There is reasonable agreement between the experimental data and the calculated priors for initial excitation of both the fundamental and overtone, which yielded essentially identical values for the excess energy of $E_{exc} = 797 \pm 100$ and 795 ± 112 cm^{-1} (2σ uncertainty). The dissociation energy of *trans*-DOOO can be calculated from the total energy available and the excess energy partitioned into the products. The energy available to the system is predominantly the energy of the IR photon used in the excitation, $h\nu_{IR}$, with an additional small contribution from the internal energy of *trans*-DOOO. In the case of initial excitation of the fundamental OD stretch, $E_{tot} = 2641$ cm^{-1} and therefore leads to $D_0 = 1844 \pm 100$ cm^{-1}. The available energy following overtone excitation is 5188 cm^{-1}, which leads to $D_0 = 1758 \pm 112$ cm^{-1}, once the vibrational energy of the $v = 1$ OD products is included in the calculation. The values agree within the experimental uncertainty; the smaller value following overtone excitation is a consequence of the anharmonicity of the OD stretch vibration in *trans*-DOOO.

A more rigorous approach to determining the dissociation energy relies on a straightforward application of energy conservation to determine a strict upper limit for D_0. The energetically highest OD $X^2\Pi$, $v = 0$ fine-structure level observed from the vibrational predissociation of *trans*-DOOO excited to ν_{OD} is the F_1, $N = 8$, f which lies at 720.36 cm^{-1}. Application of the conservation of energy leads to $D_0 \leq 1921$ cm^{-1}, and the upper limit arises from the unknown partitioning of the available energy into relative translation of the fragments and internal degrees of freedom of the O_2. The equivalent fine-structure level in $v = 1$ at 3332.42 cm^{-1} is the highest observed following dissociation of *trans*-DOOO, $2\nu_{OD}$. This reduces the upper limit for the dissociation energy still further, such that $D_0 \leq 1856$ cm^{-1}. In both cases, the upper limit derived from energy accounting is in reasonably good agreement with the prior analysis.

The OD $X^2\Pi$, $v = 1$ product state distribution in the F_1 spin−orbit manifold was also measured following excitation of the *cis*-DOOO overtone. Again, P-branch transitions showed greater in intensity than Q-branch, indicating a propensity for preferential production of $\Pi(A')$ Λ-doublets, although smaller in magnitude. The rotational distribution was slightly colder, peaking in $N = 2$ and decreasing monotonically. A prior distribution provided a reasonably good representation of the experimental data and suggests that *cis*-DOOO is of comparable stability to *trans*-DOOO.

4. Discussion

4.A. Comparisons with HOOO Spectra. The DOOO spectra observed in the OD stretch fundamental and overtone regions are almost identical to those reported previously for HOOO, aside from the large shift in the band origins upon deuteration. The line positions in the partially rotationally resolved *trans*-DOOO features are most strongly dependent on the magnitudes of the B and C rotational constants, which are only very slightly perturbed by deuteration; unsurprisingly, the heavy OOO backbone largely determines the moments of inertia. The similarities of the *trans*-DOOO and *trans*-HOOO spectra are further enforced by the identical *a*-type and *b*-type contributions to the transition dipole moments in the fundamentals and in the overtones, which indicate similar electrical anharmonicity effects in both isotopomers.

In both the protiated and deuterated species, the fundamental and overtone transitions comprise rotationally unstructured and structured bands which are attributed to the cis and trans conformers, respectively. The integrated intensities of the *cis*- and *trans*-DOOO features are also in good accord with the HOOO spectra, the unstructured cis feature making a smaller contribution to the total at the overtone than at the fundamental. The similar dissociation dynamics manifest in the product state distributions following fundamental and overtone excitation of the cis and trans features suggest that the use of action spectroscopy is not responsible for the decreasing (relative) intensity of cis with increasing vibrational excitation, rather differences in the relative oscillator strengths.

A discrepancy that remains unresolved concerns the observation of both *cis*- and *trans*-HOOO and DOOO in infrared action spectroscopy in the fundamental and overtone OH/D stretch regions, whereas only *trans*-HOOO and DOOO spectral lines were observed in the prior FTMW study of Suma et al.[16] One possible explanation is that *cis*-HOOO and DOOO lines are significantly weaker in intensity than *trans*-HOOO and DOOO lines in FTMW spectra. This possibility is supported by ab initio calculations of the permanent dipole moments of the cis and trans conformers.[39] The magnitude and direction of the permanent dipole moment for the cis conformer results in primarily *b*-type lines, but with an intensity that is ~2.5 times weaker than the corresponding *b*-type lines of the trans conformer. The orientation of the permanent dipole moment for the trans conformer results in comparable contributions from *a*- and *b*-type lines in the FTMW spectrum, as observed experimentally.[16] An alternative possibility is that the cis conformer of HOOO and DOOO is metastable relative to the trans conformer and, as a result, might be observable on the ~20 μs time scale of the infrared action spectroscopy measurements (delay between excimer photolysis and IR−UV pump−probe scheme) and not observed on the millisecond time scale typical of FTMW studies. Such metastability, e.g., due to tunneling to the trans conformer, could lead to line broadening (on the order of 10 kHz), which could degrade resolution and further reduce sensitivity for detection of the cis conformer by FTMW.

4.B. OD Product State Distributions. Vibrational predissociation of OD stretch overtone excited *trans*-DOOO was found to lead exclusively to the production of OD $X^2\Pi$, $v = 1$ products, despite the fact that $v = 0$ products are both energetically allowed and statistically preferred. The same

observation was made following overtone excitation of *trans*-HOOO.[34] This preferential loss of only a single quantum of stretch excitation during the lifetime of the vibrationally excited molecule supports the assumptions made in investigations of the kinetics of vibrational relaxation of OH $X^2\Pi$, $v > 1$ by O_2 that relaxation occurs by $\Delta v = -1$ transitions.[10–12] Vibrational predissociation following overtone excitation is the half-collision analog of relaxation via full bimolecular collisions and is consistent with the model proposed by McCabe et al.,[13] in which the rate of relaxation is controlled by the competition between IVR and dissociation of the complex. Clearly, only one quantum of OH or OD stretch excitation may be redistributed prior to dissociation.

The trends in the rotational and fine-structure distributions of the nascent OD products are also effectively identical to those observed in the analogous HOOO measurements, although some relatively subtle differences are evident. The peak in the OD rotational distributions is found to be one unit of angular momentum higher than was observed for OH but is also fairly well modeled by a prior distribution. The energetically highest observed product channel provides a rigorous upper limit for the dissociation energy of *trans*-DOOO which is $\sim$300 cm^{-1} smaller than that found for *trans*-HOOO ($D_0 \leq 2140$ cm^{-1}). Within the Born−Oppenheimer approximation, both *trans*-HOOO and *trans*-DOOO have the same D_e, but zero-point energy differences are expected to lead to different values for D_0. We shall discuss this issue in detail in a later section. There is no preference for production of either spin−orbit manifold. The apparent differences in population between F_1 and F_2 levels of a given N largely disappear after correcting for degeneracy, and the ratio is effectively unity within our experimental uncertainties. The agreement with the prior distributions further reinforces this point.

The propensity for production of $\Pi(A')$ Λ-doublets, however, is also strongly apparent in the OD $X^2\Pi$ products of *trans*-DOOO vibrational predissociation. The identification of Λ-doublets as $\Pi(A')$ or $\Pi(A'')$, corresponding to the unpaired electron residing in an orbital oriented parallel or perpendicular to the plane of molecular rotation, is strictly true only in the high-J, Hund's case b limit.[40] At low to moderate rotational levels, OD $X^2\Pi$ is more appropriately described as intermediate Hund's case a and b; thus, any given Λ-doublet is an admixture of the limiting cases. We note that the transition to case b occurs more rapidly in OH $X^2\Pi$ than in OD $X^2\Pi$ as a consequence of the smaller ratio of the spin−orbit coupling constant to the rotational constant.

This electronic effect is inherent to OD $X^2\Pi$ and limits the measurability of a dynamical Λ-doublet propensity. However, it can be straightforwardly calculated and taken into account.[41,42] The reduced degree of electron alignment, $(DEA)_{red}$, is the quotient of the experimentally measured population excess, defined as the fractional difference in population between the $\Pi(A')$ and $\Pi(A'')$ Λ-doublets and the electronic contribution, and is presented in Figure 4 as a function of N for the OD $X^2\Pi$, $v = 0$ and 1 vibrational predissociation products. The magnitude of $(DEA)_{red}$ is independent of rotational quantum number and, within experimental uncertainty, equal to the limiting value of +1 in both vibrational levels probed, meaning the unpaired electron in the OD $X^2\Pi$ product is in an orbital which lies in the plane of rotation. The lack of rotational dependence on the observed propensity suggests that its origin is stereochemical rather than dynamical and provides further evidence for our previous rationalization that the vibrational

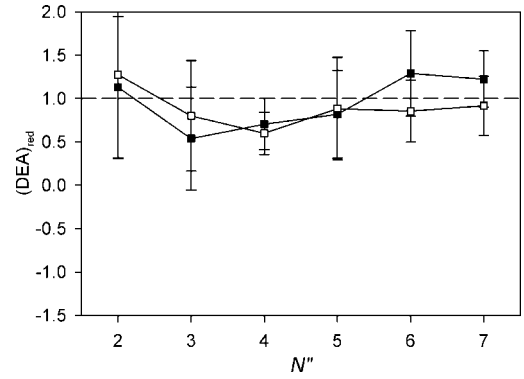

Figure 4. Reduced degree of electron alignment, $(DEA)_{red}$, observed in the OD $X^2\Pi_{3/2}$, $v = 0$ (filled squares) and $v = 1$ (open squares) products following vibrational predissociation of *trans*-DOOO excited in the OD stretch fundamental and overtone, respectively. $(DEA)_{red}$ is close to its limiting value of +1, indicating a maximal propensity for production of $\Pi(A')$ Λ-doublets, for which the unpaired electron lies in the plane of nuclear rotation.

predissociation of *trans*-HOOO and *trans*-DOOO is planar and occurs with retention of a′ symmetry of the orbital containing the unpaired electron.[34] The magnitude of $(DEA)_{red}$ observed following excitation of the *cis*-DOOO overtone was slightly smaller, again consistent with the analogous measurement on *cis*-HOOO. This may indicate that the vibrational predissociation of the cis conformer involves greater coupling to torsional motion, breaking the planarity of the dissociation.

4.C. Stability of HOOO. As discussed in the Introduction, one of the major issues of uncertainty regarding the HOOO radical is its stability relative to the OH + O_2 asymptote. The IR action spectroscopy technique used in our previous work[33,34] provided a rigorous upper limit $D_0 \leq 2140$ cm^{-1} or 6.12 kcal mol^{-1} but was limited by the increasing spacing of the rotational levels, which, furthermore, were decreasing in population for $N > 4$. The former issue is treated partially in this work, since the increased moment of inertia of OD relative to OH decreases the spacing between adjacent energy levels and thus provides a finer scale against which to measure. However, it is D_e rather than D_0 that is unchanged upon deuteration, and the DOOO upper limit of $D_0 \leq 1856$ cm^{-1} or 5.31 kcal mol^{-1} cannot be directly attributed to HOOO. Zero-point energies (ZPE) must be known if a revised D_0 for HOOO is to be calculated, as illustrated in Figure 5.

For the dissociation of DOOO

$$D_e = D_{0,D} - \Delta ZPE_D \quad (2)$$

where $D_{0,D}$ is the upper limit derived from the energetically highest observed OD product channel and ΔZPE_D is the difference in the ZPE between OD + O_2 and DOOO and is negative. An analogous expression can be written for the dissociation of HOOO, and the revised upper limit is

$$D_{0,H} = D_{0,D} - \Delta ZPE_H - \Delta ZPE_D = D_{0,D} + \Delta(\Delta ZPE) \quad (3)$$

The ZPEs of OH, OD, and O_2 can be calculated very precisely from well-characterized spectroscopic constants.[43] For polyatomic molecules calculation of ZPE requires knowledge of the harmonic vibrational frequencies, as well as the anharmonicities and all cross terms.[44] In general, these are not known, and the obvious step is to turn to ab initio or density functional methods. As commented on before, however, theoretical methods which allow harmonic and anharmonic frequency analysis generally fail to predict accurate geometries or describe the electronic structure for

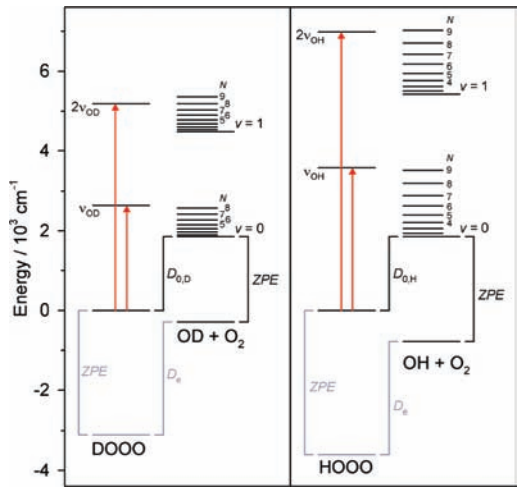

Figure 5. Left panel: Schematic illustrating the energetics of DOOO relative to the OD + O_2 asymptote. IR excitations to ν_{OD} and $2\nu_{OD}$ originate from the zero-point level of DOOO, and subsequent vibrational predissociation generates OD $X^2\Pi$ in $v = 0$ and $v = 1$, respectively. The upper limit $D_{0,D}$ derived from the energetically highest product channel is indicated. The zero-point energy (ZPE) for OD + O_2 is shown in black; that for DOOO is not known accurately, and estimated values for ZPE and D_e are indicated in gray. Right panel: Corresponding energetic diagram for the protiated system. Again, ZPE for OH and O_2 is indicated in black, while the ZPE for HOOO is estimated such that D_e is the same as in the deuterated system. It is anticipated that $D_{0,H} \leq D_{0,D}$, as discussed in the text.

HOOO. Recently, four of the five low-frequency modes of *trans*-HOOO and *trans*-DOOO have been observed in this laboratory in combination with the OH and OD stretch fundamentals and show significant discrepancies from theoretical predictions. A full analysis of the combination bands is in progress and will be presented elsewhere.[45] In the absence of reliable ZPEs, we assume that $\Delta(\Delta ZPE) \sim 0$, and the upper limit dissociation energy of HOOO can be revised downward to $D_{0,H} \leq 1856$ cm^{-1} or 5.31 kcal mol^{-1}; further refinement requires knowledge of $\Delta(\Delta ZPE)$. Qualitatively, ΔZPE_H is expected to be larger in magnitude than ΔZPE_D, since in addition to the OH stretch, the HOO bend and the HOOO torsion will shift to lower frequency upon deuteration. Consequently we anticipate that $\Delta(\Delta ZPE) \leq 0$, and a smaller dissociation energy for HOOO is most probable.

5. Conclusions

IR spectra of the OD stretch fundamental and overtone transitions of the DOOO radical have been recorded using a highly sensitive IR−UV pump−probe technique. The spectra are qualitatively similar to those observed in our previous investigations of the HOOO radical,[33,34] comprising rotationally structured bands assigned to the trans conformer and unstructured bands which are attributed to the cis conformer. Measurements of populations in rotational/fine-structure levels of the OD $X^2\Pi$ products arising from vibrational predissociation of the excited DOOO appear to be nearly statistical in their rotational and spin−orbit distributions but exhibit a strongly nonstatistical propensity for production of $\Pi(A')$ Λ-doublets. This is interpreted as indicating a planar dissociation in which the symmetry of the bonding orbital is maintained. The energetically highest OD $X^2\Pi$ product state observed following excitation of the overtone indicates an upper limit $D_0 \leq 1856$ cm^{-1} or 5.31 kcal mol^{-1} for DOOO, and this value is also adopted for HOOO, pending improved knowledge of the ZPEs.

Acknowledgment. This work was supported by the Chemistry Division of the National Science Foundation. C.M. acknowledges financial support from the Dreyfus Postdoctoral Program in Environmental Chemistry. We acknowledge the contribution of Robin Lefkowitz during the collection of some experimental data.

References and Notes

(1) Wentworth, P., Jr.; Wentworth, A. D.; Zhu, X.; Wilson, I. A.; Janda, K. D.; Eschenmoser, A.; Lerner, R. A. *Proc. Natl. Acad. Sci. U.S.A.* **2003**, *100*, 1490.
(2) Datta, D.; Vaidehi, N.; Xu, X.; Goddard, W. A. *Proc. Natl. Acad. Sci. U.S.A.* **2002**, *99*, 2636.
(3) Plesničar, B.; Cerkovnik, J.; Tekavec, T.; Koller, J. *J. Am. Chem. Soc.* **1998**, *120*, 8005.
(4) Plesničar, B.; Cerkovnik, J.; Tekavec, T.; Koller, J. *Chem.—Eur. J.* **2000**, *6*, 809.
(5) Plesničar, B.; Tuttle, T.; Cerkovnik, J.; Koller, J.; Cremer, D. *J. Am. Chem. Soc.* **2003**, *125*, 11553.
(6) Xu, X.; Goddard, W. A. *Proc. Natl. Acad. Sci. U.S.A.* **2002**, *99*, 15308.
(7) Charters, P. E.; Macdonald, R. G.; Polanyi, J. C. *Appl. Opt.* **1970**, *10*, 1747.
(8) Klenerman, D.; Smith, I. W. M. *J. Chem. Soc., Faraday Trans.* **1987**, *83*, 229.
(9) Wayne, R. P. *Chemistry of Atmospheres*, 3rd ed.; Oxford University Press: New York, 2000.
(10) Dodd, J. A.; Lipson, S. J.; Blumberg, W. A. M. *J. Chem. Phys.* **1990**, *92*, 3387.
(11) Dodd, J. A.; Lipson, S. J.; Blumberg, W. A. M. *J. Chem. Phys.* **1991**, *95*, 5752.
(12) D'Ottone, L.; Bauer, D.; Campuzano-Jost, P.; Fardy, M.; Hynes, A. J. *Phys. Chem. Chem. Phys.* **2004**, *6*, 4276.
(13) McCabe, D. C.; Smith, I. W. M.; Rajakumar, B.; Ravishankara, A. R. *Chem. Phys. Lett.* **2006**, *421*, 111.
(14) Cacace, F.; De Petris, G.; Pepi, F.; Troiani, A. *Science* **1999**, *285*, 81.
(15) Mathisen, K. B.; Siegbahn, P. E. M. *Chem. Phys.* **1984**, *90*, 225.
(16) Suma, K.; Sumiyoshi, Y.; Endo, Y. *Science* **2005**, *308*, 1885.
(17) Blint, R. J.; Newton, M. D. *J. Chem. Phys.* **1973**, *59*, 6220.
(18) Chen, M. M. L.; Wetmore, R. W.; Schaefer, H. F., III *J. Chem. Phys.* **1981**, *74*, 2938.
(19) Dupuis, M.; Fitzgerald, G.; Hammond, B.; Lester, W. A., Jr.; Schaefer, H. F., III *J. Chem. Phys.* **1986**, *84*, 2691.
(20) Chalmet, S.; Ruiz-López, M. F. *ChemPhysChem* **2006**, *7*, 463.
(21) Denis, P. A.; Kieninger, M.; Ventura, O. N.; Cachau, R. E.; Diercksen, G. H. F. *Chem. Phys. Lett.* **2002**, *365*, 440; Erratum. *Chem. Phys. Lett.* **2003**, *377*, 483
(22) Fabian, W. M. F.; Kalcher, J.; Janoschek, R. *Theor. Chem. Acc.* **2005**, *114*, 182.
(23) Jungkamp, T. P. W.; Seinfeld, J. H. *Chem. Phys. Lett.* **1996**, *257*, 15.
(24) Setokuchi, O.; Sato, M.; Matuzawa, S. *J. Phys. Chem. A* **2000**, *104*, 3204.
(25) Yang, J.; Li, Q. S.; Zhang, S. *Phys. Chem. Chem. Phys.* **2007**, *9*, 466.
(26) Yu, H. G.; Varandas, A. J. C. *Chem. Phys. Lett.* **2001**, *334*, 173.
(27) Mansergas, A.; Anglada, J. M.; Olivella, S.; Ruiz-López, M. F.; Martins-Costa, M. *Phys. Chem. Chem. Phys.* **2007**, *9*, 5865.
(28) Cooper, P. D.; Moore, M. H.; Hudson, R. L. *J. Phys. Chem. A* **2006**, *110*, 7985.
(29) Zheng, W.; Jewitt, D.; Kaiser, R. I. *Phys. Chem. Chem. Phys.* **2007**, *9*, 2556.
(30) Nelander, B.; Engdahl, A.; Svensson, T. *Chem. Phys. Lett.* **2000**, *332*, 403; Erratum. *Chem. Phys. Lett.* **2001**, *339*, 295.
(31) Speranza, M. *Inorg. Chem.* **1996**, *35*, 6140.
(32) Speranza, M. *J. Phys. Chem. A* **1998**, *102*, 7535.
(33) Murray, C.; Derro, E. L.; Sechler, T. D.; Lester, M. I. *J. Phys. Chem. A* **2007**, *111*, 4727.
(34) Derro, E. L.; Murray, C.; Sechler, T. D.; Lester, M. I. *J. Phys. Chem. A* **2007**, *111*, 11592.
(35) Colin, R.; Coheur, P.-F.; Kiseleva, M.; Vandaele, A. C.; Bernath, P. F. *J. Mol. Spectrosc.* **2002**, *214*, 225.
(36) Clyne, M. A. A.; Coxon, J. A.; Fat, A. R. W. *J. Mol. Spectrosc.* **1973**, *46*, 146.
(37) Pickett, H. M. *J. Mol. Spectrosc.* **1991**, *148*, 371.
(38) Cleary, P. A.; Dempsey, L. P.; Murray, C.; Lester, M. I.; Kłos, J.; Alexander, M. H. *J. Chem. Phys.* **2007**, *126*, 204316.
(39) Endo, Y. University of Tokyo. Personal communication, 2007.
(40) Alexander, M. H.; Andresen, P.; Bacis, R.; Bersohn, R.; Comes, F. J.; Dagdigian, P. J.; Dixon, R. N.; Field, R. W.; Flynn, G. W.; Gericke, K.-H.; Grant, E. R.; Howard, B. J.; Huber, J. R.; King, D. S.; Kinsey, J. L.; Kleinermanns, K.; Kuchitsu, K.; Luntz, A. C.; McCaffery, A. J.; Pouilly,

B.; Reisler, H.; Rosenwaks, S.; Rothe, E. W.; Shapiro, M.; Simons, J. P.; Vasudev, R.; Wiesenfeld, J. R.; Wittig, C.; Zare, R. N. *J. Chem. Phys.* **1988**, *89*, 1749.

(41) Andresen, P.; Rothe, E. W. *J. Chem. Phys.* **1985**, *82*, 3634.

(42) Macdonald, R. G.; Liu, K. *J. Chem. Phys.* **1989**, *91*, 821.

(43) Irikura, K. K. *J. Phys. Chem. Ref. Data* **2007**, *36*, 389.

(44) Wilson, E. B.; Decius, J. C.; Cross, P. C. *Molecular Vibrations*; Dover Publications, Inc.: New York, 1955.

(45) Derro, E. L.; Sechler, T. D.; Murray C.; Lester M. I. *J. Chem. Phys.* submitted for publication, 2008.

JP801232A